Proceedings of the 2007 IEEE
International Conference on Mechatronics and Automation
August 5 - 8, 2007, Harbin, China

Path Following: Discrete Stable Control of Mobile Robots

Humberto A. Secchi and Vicente A. Mut

Instituto de Automática - INAUT - Universidad Nacional de San Juan
Av. San Martín Oeste 1109 - San Juan(5400) - Argentina
hsecchi@inaut.unsj.edu.ar or hsecchi@ieee.org

***Abstract* — This paper is based on a previous work [1]. In this paper, mobile robot discrete control laws for path following, including obstacle avoidance based on distance sensorial information are developed. The mobile robot is assumed to evolve in a semi-structured environment. The paper includes the stability analysis of the developed control systems, using positive definite potential functions in discrete time. The control systems to obstacle avoidance are based on the use of the extended impedance concept. The control algorithms also avoid the potential problem of control command saturation. The performance test of control algorithms through experiences on a real mobile robot is proved.**

Keywords* — *mobile robot motion-planning; nonlinear systems; discrete time systems.

I. Introduction

Mobile robots are mechanical devices capable of moving in an environment with a certain degree of autonomy. The environment can be classified as structured when it is well known and the motion can be planned in advance, or as partially structured when there are uncertainties which imply some on-line planning of the motions. During the movement in partially structured environments, an obstacle can suddenly appear on the robot trajectory. Then, a sensorial system should detect the obstacle, measure its distance and orientation to calculate a control action to change the robot trajectory, thus avoiding the obstacle. Most works in this area consider the motion control of the mobile robot avoiding obstacles [2], [3], [4], [5] and [6], but few of them [7] study the stability of the control system problem. However, stability theoretical analysis are made in continuous domain but algorithms are implemented on real robots with discrete-time hardware and, in the same sense, the control command saturation is not taken into account.

The control architecture here presented combines two feedback loops: a motion control loop [8] and a second external impedance control loop [9]. This last loop provides a modification on target position when an obstacle appears on the trajectory of the mobile robot [10]. In this article, the concept of generalized impedance is used which relates fictitious forces to vehicle motion. Fictitious forces are calculated as a function of the measured distances. A similar concept for a generalized spring effect in robot manipulators is presented in [11]. An application of the impedance concept to avoid obstacles with robot manipulators has been presented in [12].

Main contributions of this paper are the design of discrete stable motion control laws that include the actuators saturation problem; the design of a motion control structure for obstacle avoidance and its corresponding stability analysis; and the performance test of control algorithms through experiences on a real mobile robot.

The paper is organized as follows. After this introductory section, Section 2 describes the kinematic equations of an experimental robot; Section 3 presents the control problem formulation; Section 4 defines the fictitious force for distance feedback; Section 5 presents the proposed control algorithms including their stability analysis; Section 6 is a brief survey of the mechanical characteristics and sensor capabilities of the experimental robot used; Section 7 describes the experimental results; and finally, Section 8 contains the main conclusions of the work.

II. Kinematics Equations

Consider the unicycle-like robot positioned at a non-zero distance from a goal frame $\{\mathbf{R_P}\}$. Its motion towards $\{\mathbf{R_P}\}$ is governed by the combined action of both the angular velocity ω and the linear velocity vector $\mathbf{u}$, which is always on the same direction as one of the axes of the frame $\{\mathbf{R_C}\}$ attached to the robot, as depicted in Fig. 1.

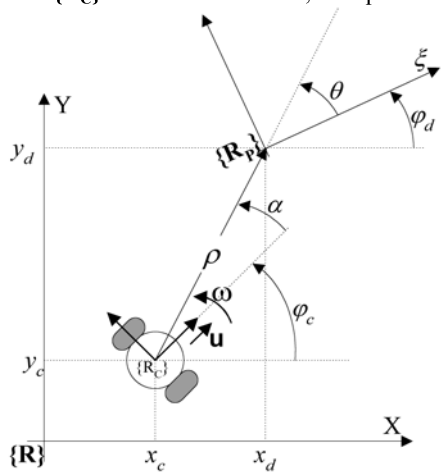

Fig. 1. Position and orientation of the vehicle.

Then, the usual set of kinematic equations in discrete-time, which involves the Cartesian position (x_C,y_C) of the vehicle and its orientation angle φ_C, is

$$\begin{cases} x_{c(k+1)} = x_{c(k)} + u_{(k)} \cdot T_0 \cdot \cos\varphi_{c(k)} \\ y_{c(k+1)} = y_{c(k)} + u_{(k)} \cdot T_0 \cdot \sin\varphi_{c(k)} \\ \varphi_{c(k+1)} = \varphi_{c(k)} + T_0 \cdot \omega_{(k)} \end{cases} \quad (1)$$

where $u_{(k)}$ and $\omega_{(k)}$ is the magnitude of $\mathbf{u}$ and ω respectively, x_C, y_C and φ_C are measured with respect to the origin of target frame $\{\mathbf{R}\}$ and to the orientation of the X-axis, and T_0 is the sample time.

Now, by representing the vehicle position in polar coordinates, and by considering the error vector ρ with orientation θ respecting

the ξ-axis of frame $\{\mathbf{R_P}\}$, as well as by letting $\alpha = \theta - \varphi_C$ be the angle measured between the main vehicle axis and the distance vector ρ, the above kinematic equations can be re-written [7]as

$$\begin{cases} \rho_{(k+1)} = \rho_{(k)} - u_{(k)} \cdot T_0 \cdot \cos\alpha_{(k)} \\ \alpha_{(k+1)} = \alpha_{(k+1)} - \omega_{(k)} \cdot T_0 + u_{(k)} \cdot T_0 \cdot \dfrac{\sin\alpha_{(k)}}{\rho_{(k)}} \\ \theta_{(k+1)} = \theta_{(k)} + u_{(k)} \cdot T_0 \cdot \dfrac{\sin\alpha_{(k)}}{\rho_{(k)}} \end{cases} \quad (2)$$

The relation between both Cartesian coordinates systems and polar coordinates systems is given as Eqn. (3)

$$\begin{cases} \rho = \sqrt{(x_d - x_c)^2 + (y_d - y_c)^2} \\ \theta = \arctan 3[(y_d - y_c),(x_d - x_c)] - \varphi_d \\ \alpha = \arctan 3[(y_d - y_c),(x_d - x_c)] - \varphi_c \end{cases} \quad (3)$$

where *arctan*3 is the arc tangent function that covers a 2π range angle in positive and negative directions and xd, yd, φd is the pose of the goal frame $\{\mathbf{R_P}\}$ respect to the inertial frame $\{\mathbf{R}\}$.

III. Problem Formulation

Let us consider the kinematic model of the mobile robot given as Eqn. (2). The main characteristics of the control problem are:

1. The objective to be reached by the mobile robot (the target frame $\{\mathbf{R_P}\}$). The control problem that will be addressed corresponds to the requirement, for the mobile robot, of approximately following an assigned directed path, by approaching it from an initial frame tangently located on the path, as indicated in Fig 2.
2. The dynamic relationship (mechanical impedance) between the position error and the interaction force **F** acting on the mobile robot. In this paper, **F** is a fictitious force generated from the distance information coming from the exteroceptive sensors (ultrasonic sensors).

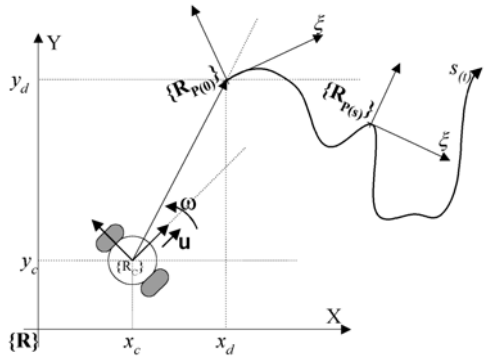

Fig. 2. Path following problem.

The problem is studied in two steps. First, when de target frame is static (pose control) and then, when the same is moving on the path (path following). Then, the problem of motion control corresponds to the design of a controller that drives the mobile robot (the unicycle-like vehicle) to the point of coordinates $\rho=0$, $\alpha=0$ and $\theta=0$ starting from any non zero distance from the target frame $\{\mathbf{R_P}\}$. In addition the problem of impedance control corresponds to the design of a controller that, after detecting obstacles in the working environment of the robot, it momentarily modifies the target position in order to avoid these obstacles.

Figure 3 represents the block diagram of the proposed control system, where, in Cartesian coordinates,

x_d, y_d, ϕ_d, is the desired position vector ;
ψ is the transformation factor vector;
$\tilde{\zeta}$ is the position error;
$\tilde{\zeta}_n$ is the modified position error.

IV. Sensorial Distance Feedback

The regulation of the mechanical impedance needs some feedback of the interaction force between the robot and the environment. Interaction forces imply a physical contact with the environment, which, in the case of mobile robots, generally represents a collision. In order to avoid obstacles, it is necessary to interact with the obstacles without causing any collision. Thus, the interaction force **F** is represented by a fictitious force generated as a function of the robot - obstacle distance, as shown in Fig. 4. The force **F** have two components: F_F is the front component and F_L is the lateral component.

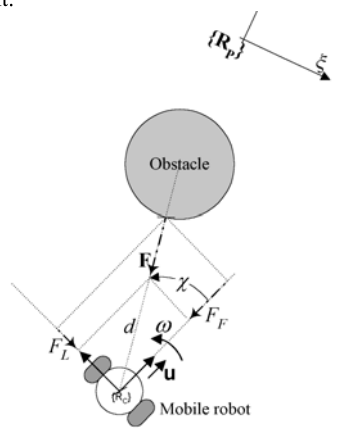

Fig. 4. Action of the fictitious force **F** on the mobile robot.

The trajectory change associated to the obstacle avoidance is performed by using the impedance concept, for which the mechanical

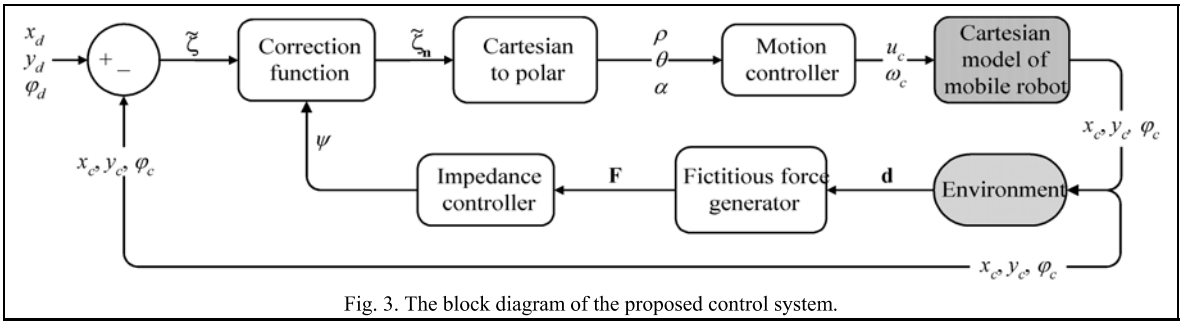

Fig. 3. The block diagram of the proposed control system.

interaction has been substituted by a distance and a non-contact interaction by taking into account the distance from the robot to the detected obstacle [12].

The magnitude of force **F** is computed as [6]

$$F_{(k)} = a - b \cdot (d_{(k)} - d_{\min})^n \quad \text{with } n = 4 \tag{4}$$

where

- *a, b* are positive constants, such that $a - b \cdot (d_{\max} - d_{\min})^n = 0$
- d_{max} is the maximum robot-obstacle distance measured by the sensorial system;
- d_{min} is the minimum robot-obstacle distance measured by the sensorial system;
- $d_{(k)}$ is the robot-obstacle distance ($d_{min} < d_{(k)} < d_{max}$);
- *n* is the sensibility of fictitious forces generator. The factor *n*=4 gives a good sensibility and allows a quick obstacle detection.

V. Control Algorithms

Two typical problems when implementing a controller are that of the practical range of control actions and its stability in the discrete temporal space. If the first is not considered in the theoretical design, possible saturation of actuators will occur and. If the second is not considered, possible disagreement between the theorical and practical stability will occur. In such a cases, the design performance of the control system can not be guaranteed to be attained. In this section controller saturation is taken into account without much computing effort. Out of the three variables ρ, α and θ, the former is considered critical in terms of saturation because it directly affects the linear velocity *u*. Finally, the stability analysis is studied and guaranteed from a point of view of the discretization of the continuous variables. Therefor, if $V_{(t)} = q_{(t)}^2$ and $\dot{V}_{(t)} = 2 \cdot q_{(t)} \cdot \dot{q}_{(t)}$ are the Lyapunov candidate function and its derivate in continuous time, then same expressions in discrete time will be $V_{(k)} = q_{(k)}^2$ and $V_{(k+1)} - V_{(k)} = 2 \cdot q_{(k)} \cdot (q_{(k+1)} - q_{(k)})$.

A. Motion Control I : Pose Control

Let the unicycle-like vehicle be initially positioned at any non-zero distance from the target frame **{R$_P$}** and let the state variables be ρ, θ and α, which are directly measurable for any ρ>*0*. Let us consider the Lyapunov candidate function

$$V_{(k)} = \frac{1}{2} \cdot h_1 \cdot \rho_{(k)}^2 + \frac{1}{2} \cdot \alpha_{(k)}^2 + \frac{1}{2} \cdot h_2 \cdot \theta_{(k)}^2 \tag{5}$$

with h_1, h_2>0. Its discrete time derivate written as the difference equation $[V_{(k+1)} - V_{(k)}]$ along the trajectory described in (2) is given as

$$\begin{aligned} V_{(k+1)} - V_{(k)} &= h_1 \cdot \rho_{(k)} \cdot (\rho_{(k+1)} - \rho_{(k)}) \\ &\quad + \alpha_{(k)} \cdot (\alpha_{(k+1)} - \alpha_{(k)}) + h_2 \cdot \theta_{(k)} \cdot (\theta_{(k+1)} - \theta_{(k)}) \\ V_{(k+1)} - V_{(k)} &= -u_{(k)} \cdot h_1 \cdot T_0 \cdot \rho_{(k)} \cdot \cos\alpha_{(k)} \\ &\quad - \omega_{(k)} \cdot \alpha_{(k)} \cdot T_0 + u_{(k)} \cdot \alpha_{(k)} \cdot T_0 \cdot \frac{\sin\alpha_{(k)}}{\rho_{(k)}} \\ &\quad - h_2 \cdot T_0 \cdot u_{(k)} \cdot \theta_{(k)} \cdot \frac{\sin\alpha_{(k)}}{\rho_{(k)}} \end{aligned} \tag{6}$$

The first term in (6) can be non-positive by letting the linear velocity *u* have the smooth form

$$u_{(k)} = \gamma_1 \cdot \tanh \rho_{(k)} \cdot \cos\alpha_{(k)} \quad \text{with } \gamma_1 > 0 \tag{7}$$

where $\gamma_1 = |u_{\max}|$. According to velocity *u* in (7), $[V_{(k+1)} - V_{(k)}]$ in (6) becomes

$$\begin{aligned} V_{(k+1)} - V_{(k)} &= -\gamma_1 \cdot h_1 \cdot T_0 \cdot \rho_{(k)} \cdot \tanh \rho_{(k)} \cdot \cos^2 \alpha_{(k)} \\ &\quad - \omega_{(k)} \cdot \alpha_{(k)} \cdot T_0 + \gamma_1 \cdot T_0 \cdot \frac{\tanh \rho_{(k)}}{\rho_{(k)}} \cdot \alpha_{(k)} \cdot \sin\alpha_{(k)} \cdot \cos\alpha_{(k)} \\ &\quad - h_2 \cdot \gamma_1 \cdot T_0 \cdot \frac{\tanh \rho_{(k)}}{\rho_{(k)}} \cdot \theta_{(k)} \cdot \sin\alpha_{(k)} \cdot \cos\alpha_{(k)} \end{aligned} \tag{8}$$

which can also be made non-positive by letting the angular velocity ω have the smooth form

$$\begin{aligned} \omega_{(k)} &= \gamma_2 \cdot \tanh\alpha_{(k)} + \gamma_3 \cdot \frac{\tanh^2 \theta_{(k)}}{\alpha_{(k)}} \\ &\quad + \gamma_1 \cdot \frac{\tanh \rho_{(k)}}{\rho_{(k)}} \cdot \sin\alpha_{(k)} \cdot \cos\alpha_{(k)} \\ &\quad + h_2 \cdot \gamma_1 \cdot \frac{\tanh \rho_{(k)}}{\rho_{(k)}} \cdot \theta_{(k)} \cdot \frac{\sin\alpha_{(k)}}{\alpha_{(k)}} \cdot \cos\alpha_{(k)} \end{aligned} \tag{9}$$

with γ_2, γ_3>0.

Where $|\omega_{\max}| = \gamma_2 + \gamma_3 + \gamma_1 \cdot 0.5 + h_2 \cdot \gamma_1 \cdot \pi$; and thus leading to the following expression for the difference equation of the original global Lyapunov function

$$\begin{aligned} V_{(k+1)} - V_{(k)} &= -h_1 \cdot \gamma_1 \cdot T_0 \cdot \rho_{(k)} \cdot \tanh\rho_{(k)} \cdot \cos^2 \alpha_{(k)} \\ &\quad - \gamma_2 \cdot T_0 \cdot \alpha_{(k)} \cdot \tanh\alpha_{(k)} - \gamma_3 \cdot T_0 \cdot \tanh^2 \theta_{(k)} < 0 \end{aligned}$$

$$\Delta V(\rho,\alpha,\theta) < 0 \Rightarrow \{\rho(k),\alpha(k),\theta(k)\} \to 0 \text{ with } k \to \infty$$

which results in a negative definite form. This means that the state variables asymptotically converge to zero when accomplishing of the control objective.

The control action of Eqn. (9) cannot be implemented for α =0 . To avoid this problem, we propose the use of a lower bound for this variable in the first term of (9). Now, it is necessary to verify that the stability conditions are kept.

By adding and subtracting the term $\left(\gamma_3 \cdot {}^{\tanh^2 \theta_{(k)}}\!/_{\alpha_0}\right)$, where $\alpha_0 = \delta_\alpha \cdot \text{sign}(\alpha_{(k)})$, $\delta_\alpha > 0$, Eqn. (9) can be rewritten as

$$\omega_{(k)} = \omega_{0(k)} + \gamma_3 \cdot \tanh^2 \theta_{(k)} \cdot \left[\frac{\alpha_0 - \alpha_{(k)}}{\alpha_0 \cdot \alpha_{(k)}}\right]$$

where ω_0 is the Eqn. (9) with α_0 in the first term, and

$$\omega_{(k)} = \begin{cases} \omega_{0(k)} + \gamma_3 \cdot \tanh^2 \theta_{(k)} \cdot \left[\dfrac{\alpha_0 - \alpha_{(k)}}{\alpha_0 \cdot \alpha_{(k)}}\right] & \text{si } |\alpha_{(k)}| \geq \delta_\alpha \\ \omega_{0(k)} & \text{si } |\alpha_{(k)}| < \delta_\alpha \end{cases} \tag{10}$$

From Eqn. (10), three cases can be analyzed:

Case I: $|\alpha_{(k)}| \geq \delta_\alpha$: Here α_0 is equal to $\alpha_{(k)}$, then

$$\begin{aligned} V_{(k+1)} - V_{(k)} &= -h_1 \cdot \gamma_1 \cdot T_0 \cdot \rho_{(k)} \cdot \tanh \rho_{(k)} \cdot \cos^2 \alpha_{(k)} \\ &\quad - \gamma_2 \cdot T_0 \cdot \alpha_{(k)} \cdot \tanh\alpha_{(k)} - \gamma_3 \cdot T_0 \cdot \tanh^2 \theta_{(k)} \end{aligned}$$

which leads to the situation already analyzed.

Case II : $|\alpha_{(k)}| < \delta_\alpha$ and $\alpha_{(k)} \neq 0$: Difference equation becomes

$$V_{(k+1)} - V_{(k)} = -h_1 \cdot \gamma_1 \cdot T_0 \cdot \rho_{(k)} \cdot \tanh \rho_{(k)} \cdot \cos^2 \alpha_{(k)} - \gamma_2 \cdot T_0 \cdot \alpha_{(k)} \cdot \tanh \alpha_{(k)} - \gamma_3 \cdot T_0 \cdot \tanh^2 \theta_{(k)} \cdot \frac{\alpha_{(k)}}{\alpha_0}$$

In this case $0 < \alpha_{(k)} / \alpha_0 \leq 1$, thus implying that difference equation is negative definite and asymptotic convergence of control errors to zero is again verified.

Case III : Evolution of $\theta_{(k)}$ when $\alpha_{(k)}=\alpha_{(k+1)}=0$. In this case

$$\gamma_3 \cdot T_0 \frac{\alpha_{(k)}}{\alpha_{0(k)}} \cdot \tanh^2 \theta_{(k)} = 0$$

thus, it is not evident the convergence to zero of signal $\theta_{(k)}$. We can now recall the Theorem of LaSalle for autonomous systems [13] by noting that:

1. The system is autonomous.
2. There exists a set $\mathbf{S}(\rho,\theta,\alpha) / \Delta V = (V_{(k+1)} - V_{(k)}) = 0$.
3. If $\Delta V = 0$, it means that $\alpha_{(k)} = 0$ and $\rho_{(k)} = 0$.

From Eqn. (2) in closed loop

$$\theta_{(k+1)} - \theta_{(k)} \leq \gamma_1 \cdot T_0 \cdot \sin \alpha_{(k)} \cdot \cos \alpha_{(k)}$$

when $\alpha_{(k)} = 0 \rightarrow [\theta_{(k+1)} - \theta_{(k)}] = 0$ which means $\theta_{(k)}$ is *constant.* Now constant value of $\theta_{(k)}$ in the set **S** can be obtained. From (2) in closed loop, when $\alpha_{(k)} = 0$ and $\rho_{(k)} = 0$ and consequently $\alpha_{(k+1)} = 0$

$$-\gamma_3 \cdot \frac{\tanh^2 \theta_{(k)}}{\alpha_0} - h_2 \cdot \gamma_1 \, \theta_{(k)} = 0$$

It is immediately concluded that $\theta_{(k)}$ can be zero in **S** if the constants are chosen correctly such as

$$\frac{h_2 \cdot \gamma_1 \cdot \alpha_0}{\gamma_3} > 0.8$$

According to La Salle theorem, this means that control error signals converge asymptotically to zero.

As a general conclusion and, since for the three cases the error signals converge asymptotically to zero, the control objective is guaranteed for the controller with bounded control actions.

B. Motion Control II : Path Following

By assuming the oriented path parametrized by the curvilinear abscissa $s_{(k)}$, and denoting with $\{\mathbf{R_{P(s)}}\}$ the corresponding frame tangently located on the oriented path, let us now consider the possibility of continuously moving $\{\mathbf{R_{P(s)}}\}$ from its initial position $\{\mathbf{R_{P(0)}}\}$ with a non-negative velocity $\Delta s / T_0$ to be appropriately assigned, where $\Delta s = s_{(k+1)} - s_{(k)}$.

Then, by considering $\{\mathbf{R_{P(s)}}\}$ as the current target for the robot, we can easily verify that in this case, due to the superimposed target motion, the original kinematic equations (2) modify as follows:

$$\begin{cases} \rho_{(k+1)} = \rho_{(k)} - u_{(k)} \cdot T_0 \cdot \cos \alpha_{(k)} + \Delta s_{(k+1)} \cdot \cos \theta_{(k)} \\ \alpha_{(k+1)} = \alpha_{(k)} - \omega_{(k)} \cdot T_0 + u_{(k)} \cdot T_0 \cdot \frac{\sin \alpha_{(k)}}{\rho_{(k)}} - \Delta s_{(k+1)} \cdot \frac{\sin \theta_{(k)}}{\rho_{(k)}} \\ \theta_{(k+1)} = \theta_{(k)} + u_{(k)} \cdot T_0 \cdot \frac{\sin \alpha_{(k)}}{\rho_{(k)}} - \Delta s_{(k+1)} \cdot \frac{\sin \theta_{(k)}}{\rho_{(k)}} - \frac{\Delta s_{(k+1)}}{R_{(s)}} \end{cases} \quad (11)$$

with $\rho_{(0)}>0$ and where *R(s)* is the current "signed curvature radius of the path (positive or negative depending from its location on the right or left side of the path itself) and where all the additional terms depending on Δs just represent the "perturbations" which are introduced by the assumed motion of the target. By assuming now that the control laws (7) and (10) are applied also in the present case, we immediately have that in such closed loop conditions the corresponding equations (12) become

$$\begin{cases} \rho_{(k+1)} = \rho_{(k)} - \gamma_1 \cdot \tanh \rho \cdot T_0 \cdot \cos^2 \alpha + \Delta s \cdot \cos \theta \\ \alpha_{(k+1)} = \alpha_{(k)} - \gamma_2 \cdot T_0 \cdot \tanh \alpha - \gamma_3 \cdot T_0 \cdot \frac{\tanh^2 \theta}{\alpha} \\ \qquad - h_2 \cdot \gamma_1 \cdot T_0 \cdot \frac{\tanh \rho}{\rho} \cdot \frac{\sin \alpha}{\alpha} \cdot \cos \alpha - \Delta s \cdot \frac{\sin \theta}{\rho} \\ \theta_{(k+1)} = \theta_{(k)} + \gamma_1 \cdot T_0 \cdot \frac{\tanh \rho}{\rho} u \cdot T_0 \cdot \sin \alpha \cdot \cos \alpha - \Delta s \cdot \frac{\sin \theta}{\rho} - \frac{\Delta s}{R_{(s)}} \end{cases} \quad (12)$$

where the rate $\Delta s_{(k+1)}$ now represents the sole control action which is made available for the accomplishment of the required path following task. To this aim the following closed loop policy is then proposed for the on-line specification of the target motion rate:

$$\frac{\Delta s_{(k+1)}}{T_0} = \begin{cases} 0 & V = h_1 \cdot \rho_{(k)}^2 + \left(\alpha_{(k)}^2 + h_2 \cdot \theta_{(k)}^2\right) > \varepsilon \\ f_{(\rho,\theta,\alpha)} & V = h_1 \cdot \rho_{(k)}^2 + \left(\alpha_{(k)}^2 + h_2 \cdot \theta_{(k)}^2\right) \leq \varepsilon \end{cases} \quad 0 < \varepsilon < \pi^2/4 \quad (13)$$

where $f_{(\rho,\theta,\alpha)}$ is any continuous radial function centered on the ellipsoidal domain $h_1 \cdot \rho_{(k)}^2 + \left(\alpha_{(k)}^2 + h_2 \cdot \theta_{(k)}^2\right) = \varepsilon$, which attains its maximum value (equal to the largest admissible one for $\Delta s / T_0$ in correspondence with the origin, and a null minimum value in correspondence on the border of the ellipsoid itself.

The rationale underlying the proposed policy structure for $\Delta s / T_0$ can be now explained on the basis of the following considerations:

1- When the robot state is outside the ellipsoidal domain (as it could be, for instance, during the beginning of the motion, when the mobile robot has to approach the starting frame $\{\mathbf{R_{P(0)}}\}$ the target is maintained in a fixed absolute position as specified by the first of (13), thus implying that in this case the mobile robot results in being driven by control laws (7) and (10) acting within their usual "fixed target" operating conditions. These force the state trajectory to evolve continuously in such a way to asymptotically converge toward the origin.

2- Due to such behavior, it then necessarily follows that the mobile robot state will reach the ellipsoid surface in a finite time (say ***t****).

3- Then, by noting that the rate $\Delta s / T_0$ is also zero on the whole ellipsoid surface as prescribed by $f_{(\rho,\theta,\alpha)}$ evaluated on it, and in correspondence with the reached point we actually have $\Delta V_{(k+1)} < 0$ due to $\rho>0$, we can also immediately conclude that, successive to ***t**** but connected with it, a time interval exists during which the state trajectory evolves continuously ***strictly*** inside the ellipsoid, while-still maintaining $\rho>0$.

4- Once the state is inside the ellipsoid with $\rho>0$, a non-zero positive value is consequently assigned to the rate $\Delta s / T_0$ by function $f_{(\rho,\theta,\alpha)}$ as prescribed by (13). Then, since within the ellipsoid $|\theta| < \pi / 2 \cdot \sqrt{h_2}$ and $|\alpha| < \pi/2$, it immediately follows that a positive contribution is actually added to $\rho_{(k+1)}$, as established by the first of (11). Hence, during the motion inside of the ellipsoid, the state trajectory cannot consequently reach the condition $\rho_{(k)}=0$ in a

whatever finite time; thus guaranteeing the continuity of the state trajectory evolution also within the ellipsoidal domain itself.

5- Moreover, inside the ellipsoid the function $V_{(k)}$ can not guaranteed that its increment $\Delta V_{(k+1)}$ to have a negative semi-definite form (as instead it occurs outside and on the surface of it). This induces the obvious possibility that, from the inside of such domain and within a certain time interval, the state norm might also increase continuously and in a way that can allow the state trajectory itself to eventually reach again the ellipsoid surface, by now proceeding from its internal side. If this occurs in correspondence with a time instant $k \cdot T_0$, we can again see, on the basis of the previous consideration, that it must be $\rho_{(k)}>0$ and consequently, an immediate future time interval certainly exists, where the state trajectory is compelled to locate ***inside*** the ellipsoid. The obvious consequence is that since $\Delta s / T_0$ is a non negative quantity, the curvilinear abscissa $s_{(k)}$ will be certainly a monotonically increasing function of time. Thus finally implying that the goal frame-point $\{\mathbf{R}_{\mathbf{P(s)}}\}$ will proceed monotonically along the assigned path, till its complete covering. Moreover, during its travel along the path, $\{\mathbf{R}_{\mathbf{P(s)}}\}$ will maintain the mobile robot behind of it, with an error distance and misalignment whose (squared) norms are, at each sample time, measured by the actual value assumed by the Lyapunov function $V_{(k)}$.

C. Impedance Control

In order to make the robot avoid obstacles, we use the concept of generalized impedance (Mut *et al.*, 1992). The desired impedance function is defined by the relationship

$$Z_{(z)} = B_z \cdot z + K_z \tag{14}$$

and the impedance relation is defined as

$$\boldsymbol{\Psi}_{(z)} = \begin{bmatrix} \psi_{L(z)} \\ \psi_{F(z)} \end{bmatrix} = Z_{(z)}^{-1} \cdot \begin{bmatrix} F_{(z)} \cdot sign\left(F_{L(z)}\right) \\ F_{F(z)} \end{bmatrix} \tag{15}$$

where

B_Z, K_Z	are positive constants. Constant B represents a damping effect and K a spring effect in the interaction robot-obstacle,
$F_{(Z)}$	is the magnitude of the fictitious force **F**,
$F_{F(Z)}$, $F_{L(Z)}$	are the component frontal and perpendicular to **F** respectively,
$\boldsymbol{\Psi}(Z)$	is the vector of change in the mobile robot movement objective,
$\psi_{F(Z)}$, $\psi_{L(Z)}$	are the magnitude of the component linear and angular, respectively, of $\boldsymbol{\Psi}$,

Then, the transformation

$$\tilde{\zeta}_{\mathbf{n}(k)} = \begin{bmatrix} \cos\psi_{L(k)} & \sin\psi_{L(k)} & 0 \\ -\sin\psi_{L(k)} & \cos\psi_{L(k)} & 0 \\ 0 & 0 & 1 \end{bmatrix} \cdot \frac{\tilde{\zeta}_{(k)}}{10^{\psi_{F(k)}}} \tag{16}$$

is applied. When the fictitious force is zero, $\tilde{\zeta}_{\mathbf{n}(k)} = \tilde{\zeta}_{(k)}$, and the objective of the motion control loop is achieved, meaning that $\tilde{\zeta}_{(k)} \to 0$ as $k \to \infty$.

For some object configurations, methods like the one described, which are based on repulsion forces, can drive the robot to a local minimum, thus confining it into an area far from the target position. A possible solution is to combine the controller with a Global Path Planning, which is beyond the aims of the present work.

VI. Pioneer Mobile Robot

The proposed controllers were tested on the Pioneer 2 mobile robot (see Fig. 5). Its main features are:

1. Dimensions are L: 0.44m x W: 0.33m x H: 0.22m
2. It supports both, front and rear sonar arrays, each with eight transducers for object detection and range information for feature recognition, as well as navigation around obstacles. The sonar positions are fixed in both arrays.
3. The drive system of Pioneer 2 uses high-speed, high torque, reversible DC motors. This model is a differential-drive mobile robot with a linear and rotational speed maximum of 1.6m/sec and 5.2 rad/sec, respectively.

Fig. 5. Mobile robot Pioneer 2.

VII. Experiences

In the following examples, the values u_{max}=0.3m/sec and ω_{max}=1.6rad/sec have been chosen in order to select design parameters and to avoid saturation of control actions. The parameters were set at:

γ_1=0.30	γ_2=0.65	γ_3=1·e^{-5}
γ_1=0.30	γ_2=0.40	K_Z=10
h_2=0.25	α_0=π/1000	B_Z=1.2

The tests were made in a partially structured environment, where the obstacles (columns and walls) have definite geometric forms but their positions are assumed to be unknown. The controllers guide the mobile robot from an initial position to a target position while avoiding the obstacles on its way. The obstacles are detected by the ultrasonic sensor system at a distance lees than 0.60m.

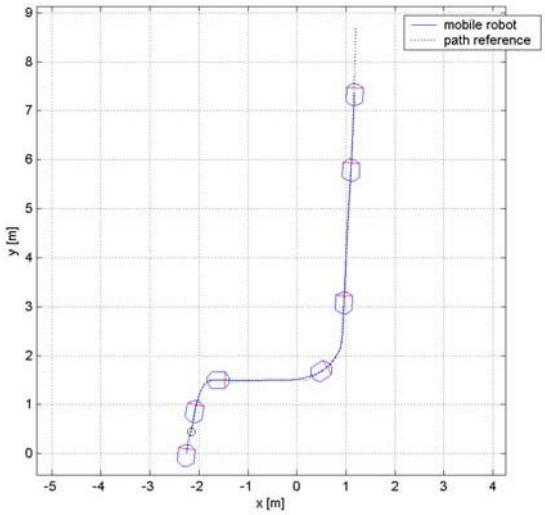

Fig. 6. Path following in free space.

Figure 6 show the trajectory described by the mobile robot in the case of path following in free space. Figure 7 show the linear and angular velocities of the mobile robot along trajectory.

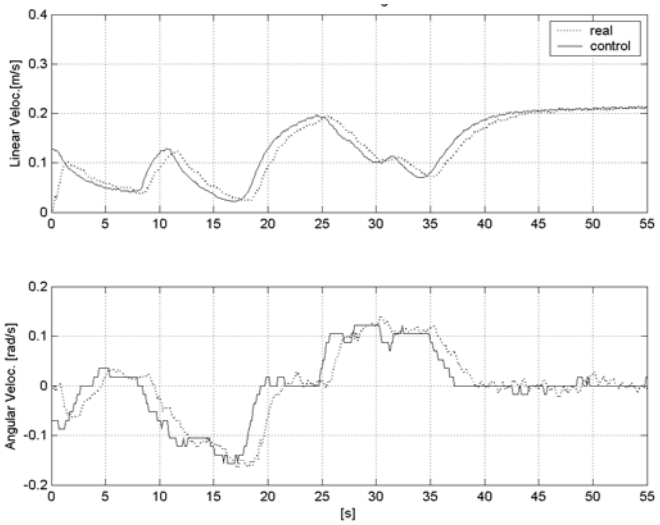

Fig. 7. Linear and angular velocities of the mobile robot in free space.

Figure 8 show the trajectory described by the mobile robot in the case of path following in the constrained space when avoiding obstacles.

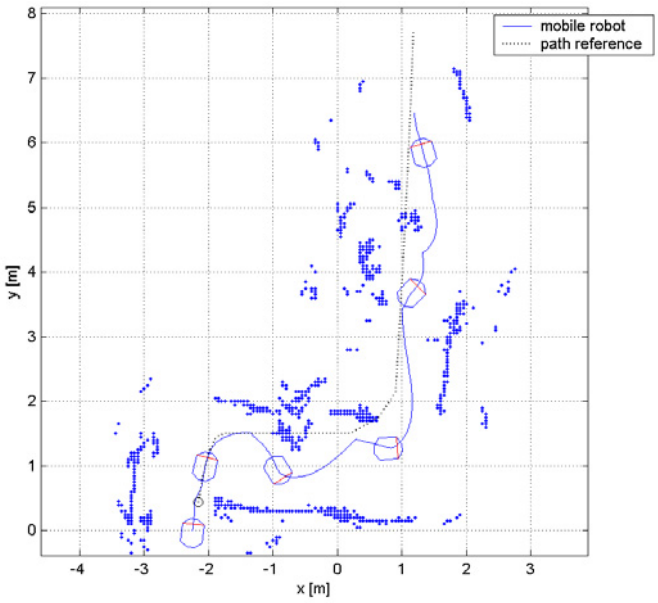

Fig. 8. Trajectory described by the mobile robot to avoid obstacles on its path.

VIII. Conclusions

This paper presents a simple and effective closed loop control law for a unicycle-like vehicle, combined with an effective control law for obstacle avoidance. First, two control objectives are considered: pose control and path following control of the vehicle. The control system is structured based on two loops, the position control loop and the impedance control loop. Impedance is defined as referred to a fictitious force, as a function of the sensed distance to any obstacle in the vicinity of the robot. The controllers keep the position error $\rho_{(k)}$ within admissible bounds in order to avoid saturation of control actions. The control system is proven to globally and asymptotically drive the control errors towards zero. Experiences have been carried out on a Pioneer mobile robot in order to show the good performance properties of the proposed control system.

References

[1] Secchi, H., R. Carelli and V. Mut, "An Experience on Stable Control of Mobile Robots". *Latin American Applied Research*. **33**, No.4, 379-385 (2003).

[2] Khatib, O. "Real-time obstacle avoidance for manipulators and mobile robots*" Proceedings IEEE-ICRA*, St. Louis MO, 500-505 (1985).

[3] Newman, W. S. and N. Hogan, "High speed robot control and obstacle avoidance using dynamic potential functions" *Proceedings IEEE-ICRA*, Raleigh NC, 14-24 (1987).

[4] Borenstein J. "Real-time obstacle avoidance for fast mobile robots" *IEEE Trans. System, Man & Cybern*., **19**, **No. 5**, 1179-1187 (1989)

[5] Koren Y. and J. Borenstein, "Potential field methods their inherent limitations for mobile robots navigation" *Proceedings IEEE-ICRA*, Sacramento CA, 1398-1404 (1991).

[6] Borenstein, J. and Y. Koren. "The vector field histogram - Fast obstacle avoidance for mobile robots". *IEEE Transactions on Robotics and Automation,* **7, No 3**, 278-288 (1991).

[7] Aicardi, M., G. Casalino, A. Bicchi and A. Balestrino. "Closed loop steering of unicycle-like vehicles via Lyapunov techniques". *IEEE Robotics & Automation Magazine.* **2, No. 1**, 27-35 (1995).

[8] Secchi, H. "Autoguided vehicles control with sensorial feedback". *Master Thesis* (in Spanish). San Juan National University Foundation. (Argentina) (1998).

[9] Hogan, N. "Impedance control an approach to manipulators" Parts I and II. *ASME Journal of Dynamics Systems, Measurement and Control*, **107**, 1-16 (1985).

[10] Secchi, H., V. Mut and R. Carelli. "Impedance control for mobile robots with sensorial feedback". *XIV National Symposium of Automatic Control – AADECA*, Argentina (in Spanish) 19-24 (1994).

[11] Sagués, C., L. Montano and J. Neira. "Guarded and compliant motions using force and proximity sensors". *Internal report,* Department of Electrical and Computing Engineering, University of Zaragoza, Spain (1990).

[12] Mut, V., R. Carelli and B. Kuchen. "Adaptive impedance control for robots with sensorial feedback". *XIII National Symposium of Automatic Control - AADECA, A*rgentina (in Spanish). **1**, 345-349 (1992).

[13] Vidyasagar M. *Nonlinear Systems Analysis,* second edition. Prentice-Hall Int. (1993).